Composite Fast-Slow MPC Design for Nonlinear Singularly Perturbed Systems

Xianzhong Chen
Dept. of Chemical and Biomolecular Engineering, University of California, Los Angeles, CA 90095

Mohsen Heidarinejad
Dept. of Electrical Engineering, University of California, Los Angeles, CA 90095

Jinfeng Liu
Dept. of Chemical and Biomolecular Engineering, University of California, Los Angeles, CA 90095

Panagiotis D. Christofides
Dept. of Chemical and Biomolecular Engineering, University of California, Los Angeles, CA 90095

Dept. of Electrical Engineering, University of California, Los Angeles, CA 90095

The design of a composite control system for nonlinear singularly perturbed systems using model predictive control (MPC) is described. Specifically, a composite control system comprised of a "fast" MPC acting to regulate the fast dynamics and a "slow" MPC acting to regulate the slow dynamics is designed. The composite MPC system uses multirate sampling of the plant state measurements, i.e., fast sampling of the fast state variables is used in the fast MPC and slow-sampling of the slow state variables is used in the slow MPC. Using singular perturbation theory, the stability and optimality of the closed-loop nonlinear singularly perturbed system are analyzed. A chemical process example which exhibits two-time-scale behavior is used to demonstrate the structure and implementation of the proposed fast–slow MPC architecture in a practical setting. © 2012 American Institute of Chemical Engineers *AIChE J*, 58: 1802–1811, 2012
Keywords: process control, optimization, simulations, process dynamics

Introduction

Time-scale multiplicity is a common feature of many chemical processes and plants of industrial interest and usually arises due to the strong coupling of physico-chemical phenomena, like slow and fast reactions, occurring at disparate time-scales. In addition to this, the dynamics of control actuation and measurement sensing systems very often adds a fast-dynamics layer in the closed-loop system. The analysis and controller design problems for multiple-time-scale systems are usually addressed within the mathematical framework of singular perturbations (e.g., Ref. 1). Within this framework, a variety of explicit controller design methods have been primarily developed for both linear and nonlinear singularly perturbed systems, ranging from optimal control [1] to geometric control (e.g., Refs. 2 and 3) and Lyapunov-based control.[4]

Over the last 25 years, model predictive control (MPC) has emerged as an important control technology for industrial process control due to its ability to provide optimal control solutions accounting explicitly for input and state constraints. In MPC, an optimization problem is solved in real-

time which takes advantage of a process model to obtain an optimal control input (piecewise constant) trajectory which minimizes an objective function subject to state and input constraints. Once the optimal input trajectory is computed, the first step is implemented by the actuators, and the rest of the trajectory is discarded and the optimization is repeated in the next sampling step. Over the last 15 years, significant efforts have been made in the development of MPC formulations with certain stability guarantees (see, for example, Ref. 5). Pertaining to the present work is the method proposed in Ref. 6 where a Lyapunov-based MPC (LMPC) design was proposed which incorporates a Lyapunov function-based constraint in the first move of the MPC optimization problem to guarantee the closed-loop stability. This LMPC design inherits the stability properties of a pre-existing Lyapunov-based explicit controller and has an explicitly characterized stability region. In the context of MPC of singularly perturbed systems, most of the efforts have been dedicated to linear systems [7] or to MPC of specific classes of two-time-scale processes.[8,9] In a recent work,[10] we studied MPC for nonlinear singularly perturbed systems where MPC is used only in the slow time-scale and the fast dynamics are assumed to be stabilizable by a "fast" explicit controller. Finally, in another recent set of papers,[11,12] MPC of two-time-scale processes described by nonlinear singularly

perturbed systems in nonstandard form (i.e., systems in which the separation of slow and fast state variables is not explicit in the original coordinates and a coordinate change should be used to obtain a singularly perturbed system in standard form) was addressed; in these works the fast dynamics are also assumed to be stabilizable by a fast explicit controller.

This work focuses on MPC of nonlinear singularly perturbed systems in standard form where the separation between the fast and slow state variables is explicit. Specifically, a composite control system comprised of a ''fast'' MPC acting to regulate the fast dynamics and a ''slow'' MPC acting to regulate the slow dynamics is designed. The composite MPC system uses multirate sampling of the plant state measurements, i.e., fast sampling of the fast state variables is used in the fast MPC and slow-sampling of the slow state variables is used in the slow MPC as well as in the fast MPC. Using singular perturbation theory, the stability and optimality of the closed-loop nonlinear singularly perturbed system are analyzed. The proposed fast–slow MPC design does not require communication between the two MPCs, and thus, it can be classified as decentralized in nature. A chemical process example which exhibits two-time-scale behavior is used to demonstrate the structure and implementation of the fast–slow MPC architecture in a practical setting. Extensive simulations are carried out to assess the performance and computational efficiency of the fast–slow MPC system.

Preliminaries

Notation. The operator $|\cdot|$ is used to denote Euclidean norm of a vector and the symbol Ω_r is used to denote the set $\Omega_r := \{x \in R^{n_x}: V(x) \le r\}$ where V is a positive definite scalar function. For any measurable (with respect to the Lebesgue measure) function $w: R_{\ge 0} \to R^l$, $\|w\|$ denotes ess.sup.$|w(t)|$, $t \ge 0$. A function $\gamma: R_{\ge 0} \to R_{\ge 0}$ is said to be of class K if it is continuous, nondecreasing, and is zero at zero. A function $\beta: R_{\ge 0} \times R_{\ge 0} \to R_{\ge 0}$ is said to be of class KL if, for each fixed t, the function $\beta(\cdot, t)$ is of class K and, for each fixed s, the function $\beta(s, \cdot)$ is nonincreasing and tends to zero at infinity. The symbol diag(v) denotes a matrix whose diagonal elements are the elements of vector v and all the other elements are zeros.

Class of nonlinear singularly perturbed systems

In this work, we focus on nonlinear singularly perturbed systems in standard form with the following state-space description

$$
\begin{aligned}
\dot{x} &= f(x, z, \epsilon, u_s, w), & x(0) &= x_0 \\
\epsilon \dot{z} &= g(x, z, \epsilon, u_f, w), & z(0) &= z_0
\end{aligned}
\tag{1}
$$

where $x \in R^n$ and $z \in R^m$ denote the vector of state variables, ϵ is a small positive parameter, $w \in R^l$ denotes the vector of disturbances and $u_s \in U \subset R^p$ and $u_f \in V \subset R^q$ are two sets of manipulated inputs. The sets U and V are nonempty convex sets which are defined as follows

$$
\begin{aligned}
U &:= \{u_{s,i}(t) : |u_{s,i}(t)| \le u_{s,i}^{max}, \ i \in [1, p]\} \\
V &:= \{u_{f,j}(t) : |u_{f,j}(t)| \le u_{f,j}^{max}, \ j \in [1, q]\}
\end{aligned}
\tag{2}
$$

where $u_{s,i}^{max}$ and $u_{f,j}^{max}$ are positive real numbers, specifying the input constraints. The disturbance vector is assumed to be absolutely continuous and bounded, i.e., $W := \{w(t) \in R^l: |w(t)| \le \theta\}$ where θ is a positive real number. Because the small

parameter ϵ multiplies the time derivative of the vector z in the system of Eq. 1, the separation of the slow and fast variables in Eq. 1 is explicit, and thus, we will refer to the vector x as the slow states and to the vector z as the fast states. We assume that the vector fields f and g are sufficiently smooth in $R^n \times R^m \times [0, \bar{\epsilon}) \times R^p \times R^l$ and $R^n \times R^m \times [0, \bar{\epsilon}) \times R^q \times R^l$, respectively, for some $\bar{\epsilon} > 0$, and that the origin is an equilibrium point of the unforced nominal system (i.e., system of Eq. 1 with $u_s = 0$, $u_f = 0$, and $w = 0$).

With respect to the control problem formulation, we assume that the fast states z are sampled continuously and their measurements are available for all time t (for example, variables for which fast sampling is possible usually include temperature, pressure and hold-ups) while the slow states x are sampled synchronously and are available at time instants indicated by the time sequence $\{t_{k \ge 0}\}$ with $t_k = t_0 + k\Delta$, $k = 0, 1, \ldots$ where t_0 is the initial time and Δ is the measurement sampling time of the slow states (for example, slowly sampled variables usually involve species concentrations). The set of manipulated inputs u_f is responsible for stabilizing the fast dynamics of Eq. 1 and for this set the control action is assumed to be computed every Δ_f, while the set of manipulated inputs u_s is evaluated every Δ_s and is responsible for stabilizing the slow dynamics and enforcing a desired level of optimal closed-loop performance. The relationship between Δ, Δ_s, and Δ_f will be discussed later.

Two-time-scale decomposition

The explicit separation of slow and fast variables in the system of Eq. 1 allows decomposing it into two separate reduced-order systems evolving in different time-scales. To proceed with such a two-time-scale decomposition and to simplify the notation of the subsequent development, we will first address the issue of controlling the fast dynamics. Because there is no assumption that the fast dynamics of Eq. 1 are asymptotically stable, we assume the existence of a fast MPC law u_f that renders the fast dynamics asymptotically stable in a sense to be made precise in Assumption 2 later. In contrast to previous approaches to u_f controller design (e.g., Ref. 1), we focus on the design of a feedback control law that does not modify the open-loop equilibrium manifold for the fast dynamics. This is in contrast to our previous work [10] where the fast feedback u_f modifies the equilibrium manifold for the fast dynamics in the closed-loop system. This implies that when we set $\epsilon = 0$ in the singularly perturbed system of Eq. 1 to derive the slow subsystem $u_f = 0$, and the resulting slow subsystem takes the form

$$
\frac{dx}{dt} = f(x, z, 0, u_s, w)
\tag{3a}
$$

$$
0 = g(x, z, 0, 0, w)
\tag{3b}
$$

Assumption 1 below is a standard requirement in singularly perturbation theory (please see, for example Ref. 1) and it is made to ensure that the system of Eq. 1 has an isolated equilibrium manifold for the fast dynamics. On this manifold, z can be expressed in terms of x and w using an algebraic expression; note that $g(x, z, 0, 0, w)$ is in this case independent of the expression of the fast feedback control law u_f. This assumption does not pose any significant limitations in practical applications but it is a necessary one in the singular perturbation framework to construct a well-defined slow subsystem.

Assumption 1. *The equation* $g(x, z, 0, 0, w) = 0$ *possesses a unique root*

$$z = \tilde{g}(x, w) \tag{4}$$

with the properties that $\tilde{g}: R^n \times R^l \rightarrow R^m$ *and its partial derivatives* $\frac{\partial \tilde{g}}{\partial x}, \frac{\partial \tilde{g}}{\partial \omega}$ *are sufficiently smooth.*

Using $z = \tilde{g}(x, w)$, we can rewrite Eq. 3 as follows

$$\frac{dx}{dt} = f(x, \tilde{g}(x, w), 0, u_s, w) =: f_s(x, u_s, w) \tag{5}$$

We will refer to the subsystem of Eq. 5 as the slow subsystem.

Introducing the fast time scale $\tau = \frac{t}{\varepsilon}$ and the deviation variable $y = z - \tilde{g}(x, w)$, we can rewrite the nonlinear singularly perturbed system of Eq. 1 as follows

$$
\begin{aligned}
\frac{dx}{d\tau} &= \varepsilon f(x, y + \tilde{g}(x, w), \varepsilon, u_s, w) \\
\frac{dy}{d\tau} &= g(x, y + \tilde{g}(x, w), \varepsilon, u_f, w) - \varepsilon \frac{\partial \tilde{g}}{\partial w} \dot{w} \\
&\quad - \varepsilon \frac{\partial \tilde{g}}{\partial x} f(x, y + \tilde{g}(x, w), \varepsilon, u_s, w)
\end{aligned} \tag{6}
$$

Setting $\varepsilon = 0$, we obtain the following fast subsystem

$$\frac{dy}{d\tau} = g(x, y + \tilde{g}(x, w), 0, u_f, w) \tag{7}$$

where x and w can be considered as "frozen" to their initial values.

Slow-fast subsystem stabilizability assumptions

We assume that there exists a Lyapunov-based sufficiently smooth control law $h_s(x) = [h_{s1}(x) \ldots h_{sp}(x)]^T$ with $u_{s,i} = h_{si}(x)$, $i = 1,\ldots,p$, which renders the origin of the nominal closed-loop slow subsystem of Eq. 5 asymptotically stable while satisfying the input constraints for all the states x inside a given stability region. Such an explicit controller can be designed using Lyapunov-based control techniques.[13,14] Using converse Lyapunov theorems,[15,13,14] this assumption implies that there exist functions $\alpha_{s,i}(\cdot)$, $i = 1,2,3$ of class K and a continuously differentiable Lyapunov function $V_s(x)$ for the nominal closed-loop slow subsystem that satisfy the following inequalities

$$
\begin{aligned}
\alpha_{s,1}(|x|) &\leq V_s(x) \leq \alpha_{s,2}(|x|) \\
\frac{\partial V_s(x)}{\partial x}(f_s(x, h_s(x), 0)) &\leq -\alpha_{s,3}(|x|) \\
h_s(x) &\in U
\end{aligned} \tag{8}
$$

for all $x \in D_s \subseteq R^n$ where D_s is an open neighborhood of the origin. We denote the region $\Omega_{\rho^s} \subseteq D_s$ as the stability region of the closed-loop slow subsystem under the Lyapunov-based controller $h_s(x)$. By continuity, the smoothness property assumed for the vector fields $f_s(x, u_s, w)$ and taking into account that the manipulated inputs $u_{s,i}$, $i = 1,\ldots,p$, and the disturbance w are bounded in convex sets, there exists a positive constant M_s such that

$$|f_s(x, u_s, w)| \leq M_s \tag{9}$$

for all $x \in \Omega_{\rho^s}$, $u_s \in U$, and $w \in W$. In addition, by the continuous differentiable property of the Lyapunov function $V_s(x)$ and the smoothness property assumed for the vector field $f_s(x, u_s, w)$, there exist positive constants L_x and L_{w_s} such that

$$
\begin{aligned}
\left| \frac{\partial V_s}{\partial x} f_s(x, u_s, w) - \frac{\partial V_s}{\partial x} f_s(x', u_s, w) \right| &\leq L_x |x - x'| \\
\left| \frac{\partial V_s}{\partial x} f_s(x, u_s, w) - \frac{\partial V_s}{\partial x} f_s(x, u_s, w') \right| &\leq L_{w_s} |w - w'|
\end{aligned} \tag{10}
$$

for all $x, x' \in \Omega_{\rho^s}$, $u_s \in U$, and $w, w' \in W$.

Assumption 2. *There exists a feedback control law* $u_f = p(x)y \in V$ *where* $p(x)$ *is a sufficiently smooth vector function of its argument, such that the origin of the closed-loop fast subsystem*

$$\frac{dy}{d\tau} = g(x, y + \tilde{g}(x, w), 0, p(x)y, w) \tag{11}$$

is globally asymptotically stable, uniformly in $x \in R^n$ *and* $w \in R^l$, *in the sense that there exists a class KL function* β_y *such that for any* $y(0) \in R^m$

$$|y(t)| \leq \beta_y \left(|y(0)|, \frac{t}{\varepsilon} \right) \tag{12}$$

for $t \geq 0$.

This assumption implies that there exist functions $\alpha_{f,i}(\cdot)$, $i = 1,2,3$ of class K and a continuously differentiable Lyapunov function $V_f(y)$ for the nominal closed-loop fast subsystem that satisfy the following inequalities

$$
\begin{aligned}
\alpha_{f,1}(|y|) &\leq V_f(x) \leq \alpha_{f,2}(|y|) \\
\frac{\partial V_f(x)}{\partial y}(g(x, y + \tilde{g}(x, w), 0, p(x)y, w)) &\leq -\alpha_{f,3}(|y|) \\
p(x)y &\in V
\end{aligned} \tag{13}
$$

for all $y \in D_f \subseteq R^m$ where D_f is an open neighborhood of the origin. We denote the region $\Omega_{\rho^f} \subseteq D_f$ as the stability region of the closed-loop fast subsystem under the nonlinear controller $p(x)y$.

By continuity, the smoothness property assumed for the vector fields $g(x,y,0,u_f,w)$ and taking into account that the manipulated inputs $u_{f,j}$, $j = 1,\ldots,q$, and the disturbance w are bounded in convex sets, there exists a positive constant M_f such that

$$|g(x, y, 0, u_f, w)| \leq M_f \tag{14}$$

for all $y \in \Omega_{\rho^f}$, $u_f \in V$, and $w \in W$. In addition, by the continuous differentiable property of the Lyapunov function $V_f(x)$ and the smoothness property assumed for the vector field $g(x,y,0,u_f, w)$, there exist positive constants L_y and L_{w_f} such that

$$
\begin{aligned}
\left| \frac{\partial V_f}{\partial y} g(x, y, 0, u_f, w) - \frac{\partial V_f}{\partial y} g(x, y', 0, u_f, w) \right| &\leq L_y |y - y'| \\
\left| \frac{\partial V_f}{\partial y} g(x, y, 0, u_f, w) - \frac{\partial V_f}{\partial y} g(x, y, 0, u_f, w') \right| &\leq L_{w_f} |w - w'|
\end{aligned} \tag{15}
$$

for all $y, y' \in \Omega_{\rho^f}$, $u_f \in V$, and $w, w' \in W$.

Fast-Slow MPC Design

The singular perturbation framework of Eq. 1 can be used to develop composite control systems where an MPC is used in the fast time scale and another MPC is used in the slow time-scale. A schematic of the proposed composite fast–slow MPC architecture is shown in Figure 1. In this case, a convenient way from a control problem formulation point of view is to design a fast-MPC that uses feedback of the deviation variable y in which case u_f is only active in the boundary layer
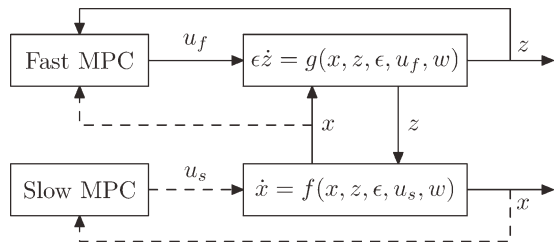
Figure 1. A schematic of the composite control system using MPC in both the fast and slow time-scales.

(fast motion of the fast dynamics) and becomes nearly zero in the slow time-scale. In this case, there is no need for communication between the fast MPC and the slow MPC (please see Remark 2 later). Specifically, referring to the singularly perturbed system of Eq. 6, the cost can be defined as

$$J = J_s + J_f = \int_0^{t_s} \left[x^T(\tilde{\tau}) Q_s x(\tilde{\tau}) + u_s^T(\tilde{\tau}) R_s u_s(\tilde{\tau}) \right] d\tilde{\tau}$$
$$+ \int_0^{t_f} \left[y^T(\tilde{\tau}) Q_f y(\tilde{\tau}) + u_f^T(\tilde{\tau}) R_f u_f(\tilde{\tau}) \right] d\tilde{\tau} \quad (16)$$

where Q_s, Q_f, R_s, R_f are positive definite weighting matrices, and t_s and t_f are the prediction horizons for the parts of the cost focusing on the slow and fast subsystems, respectively.

Lyapunov-based slow MPC formulation

Referring to the slow subsystem of Eq. 5, we use the LMPC proposed in[6] which guarantees practical stability of the closed-loop system and allows for an explicit characterization of the stability region to compute u_s. The LMPC is based on the Lyapunov-based controller $h_s(x)$. The controller $h_s(x)$ is used to define a stability constraint for the LMPC controller which guarantees that the LMPC controller inherits the stability and robustness properties of the Lyapunov-based controller $h_s(x)$. The LMPC controller is based on the following optimization problem

$$\min_{u_s \in S(\Delta_s)} \int_0^{N_s \Delta_s} \left[\tilde{x}^T(\tilde{\tau}) Q_s \tilde{x}(\tilde{\tau}) + u_s^T(\tilde{\tau}) R_s u_s(\tilde{\tau}) \right] d\tilde{\tau} \quad (17a)$$

$$\text{s.t.} \quad \dot{\tilde{x}}(\tilde{\tau}) = f_s(\tilde{x}(\tilde{\tau}), u_s, 0) \quad (17b)$$

$$u_s(\tilde{\tau}) \in U \quad (17c)$$

$$\tilde{x}(0) = x(t_k) \quad (17d)$$

$$\frac{\partial V_s(x)}{\partial x} f_s(x(t_k), u_s(0), \ 0) \leq \frac{\partial V_s(x)}{\partial x} f_s(x(t_k), h_s(x(t_k)), 0) \quad (17e)$$

where $S(\Delta_s)$ is the family of piece-wise constant functions with sampling period Δ_s, N_s is the prediction horizon, $x(t_k)$ is the state measurement obtained at t_k, $\tilde{x}$ is the predicted trajectory of the nominal system with u_s, the input trajectory computed by the LMPC of Eq. 17. The optimal solution to this optimization problem is denoted by $u_s^*(\tilde{\tau}|t_k)$, and is defined for $\tilde{\tau} \in [0, N_s \Delta_s)$. Note that in the MPC of Eq. 17, the control action is calculated every Δ_s which is the sampling interval of the slow states (i.e., $\Delta = \Delta_s$).

The optimization problem of Eq. 17 does not depend on the uncertainty and guarantees that the system in closed-loop with the LMPC controller of Eq. 17 maintains the stability

properties of the Lyapunov-based controller. The constraint of Eq. 17e guarantees that the value of the time derivative of the Lyapunov function at the initial evaluation time of the LMPC is lower or equal to the value obtained if only the Lyapunov-based controller $h_s(x)$ is implemented in the closed-loop system in a sample-and-hold fashion. This is the constraint that allows proving that the LMPC inherits the stability and robustness properties of the Lyapunov-based controller. The manipulated inputs of the closed-loop slow subsystem under the LMPC controller are defined as follows

$$u_s(t) = u_s^*(t - t_k | t_k), \quad \forall t \in [t_k, t_{k+1}) \quad (18)$$

The main property of the LMPC controller is that the origin of the closed-loop system is practically stable for all initial states inside the stability region Ω_{ρ^s} for a sufficient small sampling time Δ_s and disturbance upper bound θ. The main advantage of LMPC approaches with respect to Lyapunov-based control is that optimality considerations can be explicitly taken into account (as well as constraints on the inputs and the states[6]) in the computation of the control action within an online optimization framework.

Proposition 1 (c.f.[6,16]). *Consider the slow subsystem of Eq. 5 in closed-loop under the LMPC of Eq. 18 based on a Lyapunov-based controller $h_s(x)$ that satisfies the conditions of Eq. 8. Let $\varepsilon_{w_s} > 0$, $\Delta_s > 0$ and $\rho^s > \rho_s^s > 0$, $\theta > 0$ satisfy the following constraint*

$$-\alpha_{s,3}(\alpha_{s,2}^{-1}(\rho_s^s)) + L_x M_s \Delta_s + L_{w_s}\theta \leq -\varepsilon_{w_s}/\Delta_s \quad (19)$$

There exists a class KL function β_x and a class K function γ_x such that if $x(0) \in \Omega_{\rho^s}$, then $x(t) \in \Omega_{\rho^s}$ for all $t \geq 0$ and

$$|x(t)| \leq \beta_x(|x(0)|, t) + \gamma_x(\rho_s^*) \quad (20)$$

with $\rho_s^* = \max\{V_s(x(t + \Delta_s)) : V_s(x(t)) \leq \rho_s^s\}$.

Lyapunov-based fast MPC formulation

Referring to the fast subsystem of Eq. 7, the fast MPC at time t_k is formulated as follows

$$\min_{u_f \in S(\Delta_f)} \int_0^{N_f \Delta_f} \left[\tilde{y}^T(\hat{\tau}) Q_f \tilde{y}(\hat{\tau}) + u_f^T(\hat{\tau}) R_f u_f(\hat{\tau}) \right] d\hat{\tau} \quad (21a)$$

$$\text{s.t.} \quad \frac{d\tilde{y}}{d\hat{\tau}} = g(x(t_k), \tilde{y} + \tilde{g}(x(t_k), 0), 0, u_f, 0) \quad (21b)$$

$$u_f \in V \quad (21c)$$

$$\tilde{y}(0) = y(t_k) \quad (21d)$$

$$\frac{\partial V_f(y)}{\partial y} g(x(t_k), y(t_k) + \tilde{g}(x(t_k), 0), 0, u_f, 0)$$
$$\leq \frac{\partial V_f(y)}{\partial y} g(x(t_k), y(t_k) + \tilde{g}(x(t_k), 0), 0, p(x(t_k))y(t_k), 0) \quad (21e)$$

where $S(\Delta_f)$ is the family of piece-wise constant functions with sampling period Δ_f, N_f is the prediction horizon of this MPC, $y(t_k)$ is the state measurement obtained at t_k, $\tilde{y}$ is the predicted trajectory of the nominal system with u_f, the input trajectory computed by the LMPC of Eq. 21. The optimal solution to this optimization problem is denoted by $u_f^*(\hat{\tau}|t_k)$, and is defined for $\hat{\tau} \in [0, N_f \Delta_f)$. Note that in the MPC of Eq. 21, the control

action is calculated every Δ_f, the fast state z is available every Δ_f and the slow state x is available every Δ_s. Note also that we assume that Δ_s is an integer multiple of Δ_f.

The manipulated inputs of the closed-loop fast subsystem under the LMPC controller are defined as follows

$$u_f(t) = u_f^*(t - t_k|t_k), \quad \forall t \in [t_k, t_k + \Delta_f) \qquad (22)$$

Proposition 2 (c.f.[6,16]). *Consider the fast subsystem of Eq. 7 in closed-loop under the LMPC of Eq. 22 based on a nonlinear feedback control law $p(x)y$ that satisfies the conditions of Eq. 13. Let $\varepsilon_{w_f} > 0$, $\Delta_f > 0$ and $\rho^f > \rho_s^f > 0$, $\theta > 0$ satisfy the following constraint*

$$-\alpha_{f,3}(\alpha_{f,2}^{-1}(\rho_s^f)) + L_y M_f \Delta_f + L_{w_f}\theta \le -\varepsilon_{w_f}/\Delta_f \qquad (23)$$

Then, there exists a class KL function β_y and a class K function γ_y such that if $y(0) \in \Omega_{\rho^f}$, then $y(t) \in \Omega_{\rho^f}$ for all $t \ge 0$ and

$$|y(t)| \le \beta_y\left(|y(0)|, \frac{t}{\varepsilon}\right) + \gamma_y(\rho_f^*) \qquad (24)$$

with $\rho_f^* = \max\{V_f(y(t + \Delta_f)): V_f(y(t)) \le \rho_s^f\}$, uniformly in $x \in \Omega_{\rho^s}$ and $w \in W$.

Remark 1. *The fast LMPC of Eq. 21 utilizes feedback of the fast state vector z which is obtained continuously (fast sampling of the fast states) as well as feedback of the slow states that is available at $t_k, t_{k+1},\dots$ where $t_{k+1} = t_k + \Delta$. Because the fast MPC has to compute its control action every Δ_f, the measurement $x(t_k)$ will be used in the controller of Eq. 21 for all fast sampling times, Δ_f, within $[t_k, t_k + \Delta]$ until a new measurement of the slow state vector is obtained. Because x is practically frozen in the boundary layer - time interval in which z changes a lot but x stays nearly fixed (depending on the value of ε), - the stability of the closed-loop fast subsystem uniformly in x and w can be proved; please see also[17] and next section.*

Stability Analysis

The closed-loop stability of the system of Eq. 1 under the LMPCs of Eqs. 17 and 21 is established in the following theorem under appropriate conditions.

Theorem 1. *Consider the system of Eq. 1 in closed-loop with u_f and u_s computed by the LMPCs of Eqs. 22 and 18 based on controllers $p(x)y$ and $h_s(\cdot)$ that satisfies the conditions of Eqs. 13 and 8. Let also Assumptions 1 and 2 and the condition of Eqs. 19 and 23 hold. Then there exist functions β_x and β_y of class KL, a pair of positive real numbers (δ, d) and $\varepsilon^* > 0$ such that if $\max\{|x(0)|, |y(0)|, \|w\|\|, \|\dot{w}\|\} \le \delta$ and $\varepsilon \in (0, \varepsilon^*]$, then*

$$|x(t)| \le \beta_x(|x(0)|, t) + \gamma_x(\rho_s^*) + d$$
$$|y(t)| \le \beta_y\left(|y(0)|, \frac{t}{\varepsilon}\right) + \gamma_y(\rho_f^*) + d \qquad (25)$$

for all $t \ge 0$.

Proof: When $u_f = u_f^*$ and $u_s = u_s^*$ are determined by the LMPCs of Eqs. 22 and 18, respectively, the closed-loop system takes the following form

$$\dot{x} = f(x, z, \varepsilon, u_s^*, w), \; x(0) = x_0$$
$$\varepsilon\dot{z} = g(x, z, \varepsilon, u_f^*, w), \; z(0) = z_0 \qquad (26)$$

We will first compute the slow and fast closed-loop subsystems. Setting $\varepsilon = 0$ in Eq. 26 and taking advantage of the fact that $u_f^* = 0$ when $\varepsilon = 0$, we obtain

$$\frac{dx}{dt} = f(x, z, 0, u_s^*, w)$$
$$0 = g(x, z, 0, 0, w) \qquad (27)$$

Using that the second equation has a unique, isolated solution $z = \tilde{g}(x, w)$ (Assumption 1), we can rewrite Eq. 27 as follows

$$\frac{dx}{dt} = f(x, \tilde{g}(x, w), 0, u_s^*, w) = f_s(x, u_s^*, w) \qquad (28)$$

According to Proposition 1, the state $x(t)$ of the closed-loop slow subsystem of Eq. 28 starting from $x(0) \in \Omega_{\rho^s}$ stays in Ω_{ρ^s} (i.e., $x(t) \in \Omega_{\rho^s} \; \forall t \ge 0$) and satisfies the bound of Eq. 20.

We now turn to the fast subsystem. Using $\tau = \frac{t}{\varepsilon}$ and $y = z - \tilde{g}(x, w)$, the closed-loop system of Eq. 26 can be written as

$$\frac{dx}{d\tau} = \varepsilon f(x, y + \tilde{g}(x, w), \varepsilon, u_s^*, w)$$
$$\frac{dy}{d\tau} = g(x, y + \tilde{g}(x, w), \varepsilon, u_f^*, w)$$
$$\qquad - \varepsilon\frac{\partial\tilde{g}}{\partial w}\dot{w} - \varepsilon\frac{\partial\tilde{g}}{\partial x}f(x, y + \tilde{g}(x, w), u_s^*, w) \qquad (29)$$

Setting $\varepsilon = 0$, the following closed-loop fast subsystem is obtained

$$\frac{dy}{d\tau} = g(x, y + \tilde{g}(x, w), 0, u_f^*, w) \qquad (30)$$

According to Proposition 2, the state $y(t)$ of the closed-loop fast subsystem of Eq. 30 starting from $y(0) \in \Omega_{\rho^f}$ stays in Ω_{ρ^f} (i.e., $y(t) \in \Omega_{\rho^f} \; \forall t \ge 0$) and satisfies the bound of Eq. 24. Therefore, using similar arguments to the proof of Theorem 1 in,[17] we have that there exist functions β_x and β_y of class *KL*, positive real numbers (δ, d) (note that the existence of δ such that $|x(0)| \le \delta$ and $|y(0)| \le \delta$ imply that $x(0) \in \Omega_{\rho^s}$ and $y(0) \in \Omega_{\rho^f}$ follows from the smoothness of $V_s(x)$ and $V_f(y)$), and $\varepsilon^* > 0$ such that if $\max\{|x(0)|, |y(0)|, \|w\|, \|\dot{w}\|\} \le \delta$ and $\varepsilon \in (0, \varepsilon^*]$, then, the bounds of Eq. 25 hold for all $t \ge 0$. ∎

Remark 2. *Referring to the composite fast–slow MPC architecture of Figure 1, we note that it can find an interpretation in the context of distributed MPC architectures.[18,19,20] While conventional distributed MPC design where one MPC could manipulate u_f and another MPC could manipulate u_s would normally require the use of communication between the fast MPC and the slow MPC to coordinate their actions,[21,22] the fast-slow MPC architecture of Figure 1 takes advantage of the two-time-scale system property to design a fast-MPC that uses feedback of the deviation variable y in which case u_f is only active in the boundary layer (fast motion of the fast dynamics) and becomes nearly zero in the slow time-scale. As a result, there is no need for communication between the fast MPC and the slow MPC; in this sense, the control structure of Figure 1 can be classified as decentralized. This point demonstrates that accounting for time-scale multiplicity can lead to simplification in the communication strategy of distributed MPCs. Such a two-time-scale DMPC architecture takes advantage of the time-scale separation in the process model and yields near optimal performance in a sense to be precisely defined in the next section.*

Near Optimality

In this section, we establish that the finite-time cost of the closed-loop singularly perturbed system of Eq. 26 under the fast-slow MPCs, converges to the corresponding cost

computed on the basis of the fast and slow subsystems. It should be emphasized that the finite-time analysis of the closed-loop system optimality relies on the practical closed-loop system stability established in the previous section. We note that after the fast and slow states enter their corresponding final invariant set, we can only guarantee boundedness of the closed-loop system states but not eventual convergence to the origin. Therefore, the integral of the closed-loop cost over the infinite-time interval is infinite. As a consequence, we focus on near-optimality over a finite-time interval.

We assume $w = 0$ and define the finite-time interval $[0, t_I]$, where t_I is the time needed for the state of the closed-loop system of Eq. 26 starting from the initial condition $(x(0), z(0))$ that satisfies the conditions of Theorem 1 to enter an invariant set containing the origin in which $x(t_I) \in \Omega_{\rho_s^s}$ and $y(t_I) \in \Omega_{\rho_s^f}$. Referring to the system of Eq. 26 with $w = 0$, the finite-time cost in the time interval $[0, t_I]$ is defined as follows

$$J = J_s + J_f = \int_0^{t_I} \left[x^T(\bar{\tau}) Q_s x(\bar{\tau}) + u_s^{*T}(\bar{\tau}) R_s u_s^*(\bar{\tau}) \right] d\bar{\tau}$$
$$+ \int_0^{t_I} \left[y^T(\bar{\tau}) Q_f y(\bar{\tau}) + u_f^{*T}(\bar{\tau}) R_f u_f^*(\bar{\tau}) \right] d\bar{\tau} \quad (31)$$

where Q_s, R_s, Q_f, R_f are appropriate matrices defined in the formulation of Eqs. 17 and 21. We now define the trajectory of the closed-loop slow subsystem under the slow LMPC

$$\dot{\hat{x}} = f_s(\hat{x}, u_s^*, 0), \quad \hat{x}(0) = x_0 \quad (32)$$

for $t \in [0, t_I]$, and the corresponding cost is defined as follows

$$J_s^* = \int_0^{t_I} \left[\hat{x}^T(\bar{\tau}) Q_s \hat{x}(\bar{\tau}) + u_s^{*T}(\bar{\tau}) R_s u_s^*(\bar{\tau}) \right] d\bar{\tau} \quad (33)$$

Similarly, we define the trajectory of the closed-loop fast subsystem under the fast LMPC

$$\frac{d\hat{y}}{d\tau} = g(x, \hat{y} + \tilde{g}(x, 0), 0, u_f^*, 0), \quad \hat{y}(0) = y_0 \quad (34)$$

and the corresponding cost is defined as follows

$$J_f^* = \int_0^{t_b} \left[\hat{y}^T\left(\frac{\bar{\tau}}{\varepsilon}\right) Q_f \hat{y}\left(\frac{\bar{\tau}}{\varepsilon}\right) + u_f^{*T}\left(\frac{\bar{\tau}}{\varepsilon}\right) R_f u_f^*\left(\frac{\bar{\tau}}{\varepsilon}\right) \right] d\bar{\tau} \quad (35)$$

where t_b $\mathcal{O}(\varepsilon)$. We now state the main result of this section.

Theorem 2. *Consider the closed-loop system of Eq.* 26 *under the slow and fast LMPCs of Eqs.* 17 *and* 21, *respectively, and its corresponding slow and fast subsystems of Eqs.* 32 *and* 34. *Let* t_I *be the time needed for the state of the closed-loop system of Eq.* 26 *starting from the initial condition* $(x(0), z(0))$ *satisfying the conditions of Theorem 1 to enter an invariant set containing the origin in which* $x(t_I) \in \Omega_{\rho_s^s}$ *and* $y(t_I) \in \Omega_{\rho_s^f}$. *Then,* $J \to J_s^* + J_f^*$ *as* $\varepsilon \to 0$.

Proof. We exploit closeness of solutions results and combine them with optimality results to prove that the two-time-scale LMPC is near-optimal in the sense that the cost function associated with the full closed-loop system approaches the sum of the optimal costs of the reduced subsystems when $\varepsilon \to 0$. Using the closed-loop stability results of Eq. 25, we can obtain time t_I which is the time needed for the state of the closed-loop system of Eq. 26 starting from $(x(0), z(0))$ satisfying the conditions of Theorem 1 to enter an invariant set con-

taining the origin in which $x(t_I) \in \Omega_{\rho_s^s}$ and $y(t_I) \in \Omega_{\rho_s^f}$. Using the bound of Eq. 25 and similar arguments to the ones in the proof of Tikhonov's theorem (see Theorem 9.1 in Ref. 23), there exists $\varepsilon_0 \in (0, \varepsilon^*]$ such that $\forall \varepsilon \in (0, \varepsilon_0]$

$$x(t) = \hat{x}(t) + \mathcal{O}(\varepsilon), \quad \forall t \in [0, t_I] \quad (36)$$

$$y(t) = \hat{y}\left(\frac{t}{\varepsilon}\right) + \mathcal{O}(\varepsilon), \quad \forall t \in [0, t_I] \quad (37)$$

and

$$u_s^*(x(t)) = u_s^*(\hat{x}(t)) + \mathcal{O}(\varepsilon), \quad \forall t \in [0, t_I]$$
$$(38)$$
$$u_f^*(x(t), y(t)) = u_f^*(\hat{x}(t), \hat{y}(\tfrac{t}{\varepsilon})) + \mathcal{O}(\varepsilon), \quad \forall t \in [0, t_I]$$

From the estimates of Eqs. 36, 37, and 38, it can be concluded that there exists a positive real number $\overline{N}$ such that Eq. 31 yields

$$J = \int_0^{t_I} \left[x^T(\bar{\tau}) Q_s x(\bar{\tau}) + u_s^{*T}(x(\bar{\tau})) R_s u_s^*(x(\bar{\tau})) \right] d\bar{\tau}$$
$$+ \int_0^{t_I} \left[y^T(\bar{\tau}) Q_f y(\bar{\tau}) + u_f^{*T}(x(\bar{\tau}), y(\bar{\tau})) R_f u_f^*(x(\bar{\tau}), y(\bar{\tau})) \right] d\bar{\tau}$$
$$= \int_0^{t_I} \left[\hat{x}^T(\bar{\tau}) Q_s \hat{x}(\bar{\tau}) + u_s^{*T}(\hat{x}(\bar{\tau})) R_s u_s^*(\hat{x}(\bar{\tau})) \right] d\bar{\tau}$$
$$+ \int_0^{t_b} \left[\hat{y}^T\left(\frac{\bar{\tau}}{\varepsilon}\right) Q_f \hat{y}\left(\frac{\bar{\tau}}{\varepsilon}\right) + u_f^{*T}\left(\hat{x}(\bar{\tau}), \hat{y}\left(\frac{\bar{\tau}}{\varepsilon}\right)\right) \right.$$
$$\left. \times R_f u_f^*\left(\hat{x}(\bar{\tau}), \hat{y}\left(\frac{\bar{\tau}}{\varepsilon}\right)\right) \right] d\bar{\tau} + \bar{N}\varepsilon$$
$$= J_s^* + J_f^* + \bar{N}\varepsilon \quad (39)$$

Thus, as $\varepsilon \to 0$, we have that $J \to J_s^* + J_f^*$.

Remark 3. *Most of the literature on control of singularly perturbed systems (e.g.,* [10]) *deals with systems in which the manipulated input (or input vector),* u, *is decomposed into two components,* u_s *and* u_f, *(i.e.,* $u = u_s + u_f$*) and continuous (not sample-and-hold) implementation of the control action on the process (i.e., singularly perturbed system) is assumed. This formulation for the manipulated inputs and the control action implementation, however, is not general enough to deal with MPC as the method used for feedback design. Specifically, MPC implementation should be done in a sample-and-hold fashion, and moreover, different sampling times should be utilized by the manipulated inputs used to control the fast and slow dynamics, respectively. In particular, the manipulated inputs used to control the fast dynamics,* u_f, *should use a small sampling time, while the manipulated inputs used to control the slow dynamics,* u_s, *could use a larger sampling time. Such a difference in sampling times would not have been possible in the standard singularly perturbed control problem formulation where continuous implementation of manipulated inputs is assumed.*

Chemical Process Example

In this section, we consider a chemical process example to demonstrate the structure and implementation of the proposed fast–slow MPC architecture in a practical setting. The chemical process consists of a network of two continuously stirred tank reactors (CSTRs) and one flash tank separator with recycle. Specifically, fresh feed of species A goes into CSTR 1 through stream F_0. An elementary reaction (r_1) $A \rightarrow B$ takes place inside CSTR 1. The outlet of CSTR 1 is fed into

Table 1. Process Variables

C_{i1}, i = A,B,C D	Concentration of different species at CSTR-1
C_{i2}, i = A,B,C D	Concentration of different species at CSTR-2
C_{i3}, i = A,B,C D	Concentration of different species at CSTR-3
C_{ir}, i = A,B,C D	Concentration of different species at F_r
T_j, i = 1,2,3,r	Temperatures of CSTR-1,2,3
T_{A0},T_{C0}	Temperatures of stream F_0 and F_4
V_1, V_2 and V_3	Vessel volume of CSTR-1,2 and separator
ρ_m, ρ_{mA} and ρ_{mC}	Density of the mixture, species A and C
c_m, c_{mA} and c_{mC}	Heat capacity of the mixture, species A and C
ΔH_{r_1} and ΔH_{r_2}	Heat of reaction r_1 and r_2
k_1, and k_2	Reaction coefficients of r_1 and r_2
E_1, and E_2	Activation energy of r_1 and r_2
H_i^{vap}, i = A,B,C,D	Enthalpy of vaporization of different species

CSTR 2, where a second reaction takes place (r_2) B + C → D and produces the desired product D; note that r_2 does not take place in CSTR 1 because catalyst is not added in CSTR 1. Another stream F_4 supplies reactant C into CSTR 2 continuously. All leftover materials from CSTR 2 enter a flash separator where most of the reactants are being recycled back to CSTR 1. The dynamic equations describing the behavior of the process, obtained through material and energy balances under standard modeling assumptions, are given below

$$V_1 \frac{dC_{A1}}{dt} = F_0 C_{A0} + F_r C_{Ar} - F_1 C_{A1} - k_1 e^{-E_1/RT_1} C_{A1} V_1 \tag{40a}$$

$$V_1 \frac{dC_{B1}}{dt} = F_r C_{Br} - F_1 C_{B1} + k_1 e^{-E_1/RT_1} C_{A1} V_1 \tag{40b}$$

$$V_1 \frac{dC_{C1}}{dt} = F_r C_{Cr} - F_1 C_{C1} \tag{40c}$$

$$V_1 \frac{dC_{D1}}{dt} = F_r C_{Dr} - F_1 C_{D1} \tag{40d}$$

$$\rho_m c_{pm} V_1 \frac{dT_1}{dt} = F_0 \rho_{mA} c_{pmA} T_{A0} + F_r \rho_m c_{pm} T_3 - F_1 \rho_m c_{pm} T_1$$
$$+ (-\Delta H_{r_1}) k_1 e^{-E_1/RT_1} C_{A1} V_1 + Q_1 \tag{40e}$$

$$V_2 \frac{dC_{A2}}{dt} = F_1 C_{A1} - F_2 C_{A2} - k_1 e^{-E_1/RT_2} C_{A2} V_2 \tag{40f}$$

$$V_2 \frac{dC_{B2}}{dt} = F_1 C_{B1} - F_2 C_{B2} + k_1 e^{-E_1/RT_2}$$
$$C_{A2} V_2 - k_2 e^{-E_2/RT} C_{B2} C_{C2} V_2 \tag{40g}$$

$$V_2 \frac{dC_{C2}}{dt} = F_1 C_{C1} + F_4 C_{C0} - F_2 C_{C2} - k_2 e^{-E_2/RT_2} C_{B2} C_{C2} V_2 \tag{40h}$$

$$V_2 \frac{dC_{D2}}{dt} = F_1 C_{D1} - F_2 C_{D2} + k_2 e^{-E_2/RT_2} C_{B2} C_{C2} V_2 \tag{40i}$$

$$\rho_m c_{pm} V_2 \frac{dT_2}{dt} = F_1 \rho_m c_{pm} T_1 + F_4 \rho_{mc} c_{pmc} T_{C0}$$
$$- F_2 \rho_m c_{pm} T_2 + (-\Delta H_{r_1}) k_1 e^{-E_1/RT_2} C_{A2} V_2$$
$$+ (-\Delta H_{r_2}) k_2 e^{-E_2/RT_2} C_{B2} C_{C2} V_2 + Q_2 \tag{40j}$$

$$V_3 \frac{dC_{A3}}{dt} = F_2 C_{A2} - F_3 C_{A3} - F_r C_{Ar} \tag{40k}$$

$$V_3 \frac{dC_{B3}}{dt} = F_2 C_{B2} - F_3 C_{B3} - F_r C_{Br} \tag{40l}$$

$$V_3 \frac{dC_{C3}}{dt} = F_2 C_{C2} - F_3 C_{C3} - F_r C_{Cr} \tag{40m}$$

$$V_3 \frac{dC_{D3}}{dt} = F_2 C_{D2} - F_3 C_{D3} - F_r C_{Dr} \tag{40n}$$

$$\rho_m c_{pm} V_3 \frac{dT_3}{dt} = F_2 \rho_m c_{pm}(T_2 - T_3) - \sum_i^{A,B,C,D} F_r C_{ir} H_i^{vap} + Q_3 \tag{40o}$$

where the definitions of the the process variables and their assigned values are shown in Table 1 and Table 2, respectively.

The models of the CSTRs and of the separator are developed under the assumptions that the liquid hold-up level of all tanks is fixed and the relative volatility of each species is constant. The following algebraic equations govern the molar composition of different species at the recycle stream

$$x_{Ar} = \frac{\alpha_A C_{A3}}{\alpha_A C_{A3} + \alpha_B C_{B3} + \alpha_C C_{C3} + \alpha_D C_{D3}}$$

$$x_{Br} = \frac{\alpha_B C_{B3}}{\alpha_A C_{A3} + \alpha_B C_{B3} + \alpha_C C_{C3} + \alpha_D C_{D3}}$$

$$x_{Cr} = \frac{\alpha_C C_{C3}}{\alpha_A C_{A3} + \alpha_B C_{B3} + \alpha_C C_{C3} + \alpha_D C_{D3}}$$

$$x_{Dr} = \frac{\alpha_D C_{D3}}{\alpha_A C_{A3} + \alpha_B C_{B3} + \alpha_C C_{C3} + \alpha_D C_{D3}}$$

where x_{ir}, i = A, B, C, D represents the molar composition of species A, B, C, and D, respectively. Each of the tanks has an external heat input that is used as manipulated input, labeled as Q_1, Q_2, and Q_3. In this example, the liquid holdup V_2 in the catalytic reactor CSTR 2 is significantly smaller than the liquid holdup in CSTR 1, V_1, and the flash separator V_3.

Taking this into account, the process model of Eq. 40 can be converted into the standard singularly perturbed form by dividing Eqs. 40f–40j by V_1 and defining $\varepsilon = \frac{V_2}{V_1}$ to derive the following state-space model

$$\dot{x} = f(x, z, \varepsilon, Q_1, Q_3, w_s), \ x(0) = x_0$$
$$\varepsilon \dot{z} = g(x, z, \varepsilon, Q_2, w_f), \ z(0) = z_0 \tag{41}$$

where the fast state $z = [C_{A2} \ C_{B2} \ C_{C2} \ C_{D2} \ T_2]$ and the slow state x consists of the rest of the state variables. With respect to the manipulated input decomposition, Q_1 and Q_3 enter the slow process states, x, and will be regulated by the slow MPC, and Q_2 enters the fast process states, z, and will be regulated by the fast MPC. Finally, we define the following deviation variables $\bar{z} = z - z_{set}$ and $\bar{x} = x - x_{set}$, where z_{set} and x_{set} are the desired (final) steady-state values and are defined in Table 3.

Table 2. Process Values

V_1	4.0 m³	V_2	0.2 m³
V_3	3.0 m³	T_{A0}	298.15 K
T_{C0}	298.15 K	C_{A0}	2 kmol m⁻³
C_{C0}	2 kmol m⁻³	F_0	0.04 m³ s⁻¹
F_4	0.05 m³ s⁻¹	F_r	1.8 m³ s⁻¹
ρ_m	900.0 kg m⁻³	ρ_{mA}	950.0 kg m⁻³
ρ_{mC}	870.0 kg m⁻³	c_{pm}	0.231 kcal kg⁻¹ K⁻¹
c_{pmA}	0.214 kcal kg⁻¹ K⁻¹	c_{pmC}	0.251 kcal kg⁻¹ K⁻¹
ΔH_{r_1}	5.4 × 10¹ kcal mol⁻¹	ΔH_{r_2}	9.98 × 10¹ kcal mol⁻¹
k_1	3.35 × 10³ s⁻¹	k_2	5.25 × 10⁴ m³ kmol⁻¹ s⁻¹
E_1	1.04 × 10⁴ kcal kmol	E_2	4.0 × 10³ kcal kmol
R	1.987 kcal kmol⁻¹ K⁻¹	H_A^{vap}	100 kcal kmol⁻¹
H_B^{vap}	110 kcal kmol⁻¹	H_C^{vap}	120 kcal kmol⁻¹
H_D^{vap}	120 kcal kmol⁻¹		

Table 3. Initial Steady-State and Final Steady-State Manipulated Input Values

Initial steady state (unit kcal)		
$Q_1^{\text{int}} = 3.2e3$	$Q_2^{\text{int}} = -3.7e3$	$Q_3^{\text{int}} = 3.5e3$
Final steady-state (unit kcal)		
$Q_1^{\text{set}} = 5.2e3$	$Q_2^{\text{set}} = -4.7e3$	$Q_3^{\text{set}} = 2.8e3$

Controller synthesis

In this section, we synthesize three control schemes: (a) a centralized LMPC architecture, (b) an MPC architecture that uses a fast explicit controller and a slow LMPC,[10] and (c) the composite fast–slow LMPC architecture introduced in this article, shown in Figure 2. All controller designs have the same objective to drive the system from an initial steady-state to a final steady-state; both are stable steady-states and are defined in Table 3. In the context of the centralized LMPC, the manipulated input vector is defined as $u = [u_1 \ u_2 \ u_3]^T = [Q_1 - Q_1^{\text{set}} \ Q_2 - Q_2^{\text{set}} \ Q_3 - Q_3^{\text{set}}]^T$ for all LMPC synthesis and their constraints are chosen to be

$$3.2e3 \text{ kcal} \ \le u_1 \le 6.0e3 \text{ kcal}$$
$$-5.5e3 \text{ kcal} \ \le u_2 \le -2.8e3 \text{ kcal}$$
$$2.0e3 \text{ kcal} \ \le u_3 \le 4.0e3 \text{ kcal}$$

We consider the following objective function in the centralized LMPC design

$$J_c = \int_0^{t_l} [\bar{x}^T(\bar{\tau})Q_{c1}\bar{x}(\bar{\tau}) + \bar{z}^T(\bar{\tau})Q_{c2}\bar{z}(\bar{\tau}) + u^T(\bar{\tau})R_c u(\bar{\tau})]d\bar{\tau}$$

$$(42a)$$

where Q_{c1} and Q_{c2} are weighting matrices and their diagonal values are defined as the reciprocal of the average of the initial and final steady-state values of the states they are associated with, and $R_c = \text{diag}([1.0e-8 \ 1.0e-8 \ 1.0e-10])$ is also a weighting matrix. With respect to the Lyapunov constraint, three different proportional controllers are implemented as $h(\bar{x})$

$$u_1 = k_1(T_1^{\text{set}} - T_1) \qquad (43a)$$

$$u_2 = k_2(T_2^{\text{set}} - T_2) \qquad (43b)$$

$$u_3 = k_3(T_3^{\text{set}} - T_3) \qquad (43c)$$

where T_1^{set}, T_2^{set}, and T_3^{set} are the final steady-state temperatures of each vessel and k_1, k_2, and k_3 are constant coefficients and are chosen to be -60, 50, and 30, respectively. All diagonal elements of the weighting matrices of the Lyapunov function $V = \bar{x}^T P_1 \bar{x} + \bar{z}^T P_2 \bar{z}$ are chosen to be unity.

To synthesize the slow LMPC and the composite fast-slow LMPC schemes, we first split the set of manipulated inputs u into $u_s = [u_1 \ u_3]$ and $u_f = [u_2]$. Following from Eq. 17, the slow time-scale objective function J_s in this example is chosen to be

$$J_s = \int_0^{t_l} [\bar{x}^T(\bar{\tau})Q_{c1}\bar{x}(\bar{\tau}) + u_s^T(\bar{\tau})R_s u_s(\bar{\tau})]d\bar{\tau} \qquad (44)$$

where R_s has the same values as in R_c for the same input variables. To solve for Eq. 17c, the nonlinear algebraic equation $g(\bar{x}, w)$ has to be solved at each slow sampling time when the slow state measurements are available. The Lyapunov based controller $h_s(\bar{x})$ in the slow LMPC design implements the same

proportional control law as in Eqs. 43a,c. To complete the synthesis of the slow LMPC scheme, we assign the slow LMPC to regulate the heat inputs Q_1 and Q_3 and assign the proportional controller Eq. 43b to regulate the heat input Q_2.

Finally, we use the following objective function J_f for the fast LMPC

$$J_f = \int_0^{t_l} [y^T(\bar{\tau})Q_{c2}y(\bar{\tau}) + u_f^T(\bar{\tau})R_f u_f(\bar{\tau})]d\tau \qquad (45)$$

where $R_f = 1.0e-8$ and y is defined as $y = \bar{z} - g(\bar{x}, w)$. The formulation of fast LMPC requires that the nonlinear function $g(\bar{x}, w)$ has to be solved at the end of each fast sampling time where the slow state measurements are available. The controller $p(\bar{x})y$ appeared on the Lyapunov constraint at Eq. 21e is designed to be a control law of the form $p(\bar{x})y = k_4(g(\bar{x}, w) - T_2)$ where $k_4 = 25$. Together with the slow LMPC design, this completes the synthesis of the composite fast-slow LMPC.

Closed-Loop Results

The simulations are performed in C++ programming environment by a Core2 Quad Q6600 computer. The simulation time for each run is 510 seconds. We study the closed-loop system stability and performance of each of the MPC schemes, and by comparison, we evaluate the characteristics of the composite fast-slow LMPC design in terms of stability, optimality and control action evaluation time.

For all simulation studies, we use the same prediction horizon $N = 1$. The fast and slow state measurements are assumed to be available at every three seconds ($\Delta = 3$ sec) to all LMPC controllers, and the temperature measurement (T_2) is assumed to be continuously available to the proportional controller used in the slow LMPC design that utilizes a fast proportional controller. The initial time where all state measurements are available is $t = 0$ sec. The sampling times of the centralized LMPC, slow LMPC and fast LMPC are $\Delta_c = 15$ sec, $\Delta_s = 15$ sec, and $\Delta_f = 3$ sec, respectively; note that the measurement sampling time Δ is equal to Δ_f. For each LMPC scheme, only the first step from the computed optimal input trajectory of the optimization problems is implemented in each sampling time following a receding horizon scheme. The manipulated input regulated by the proportional
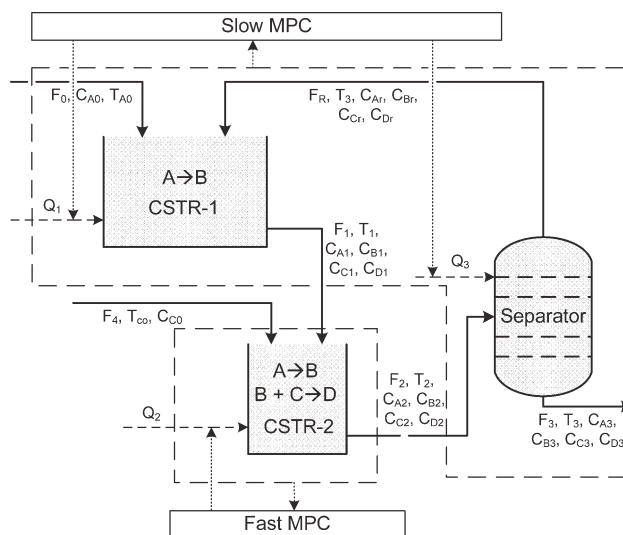

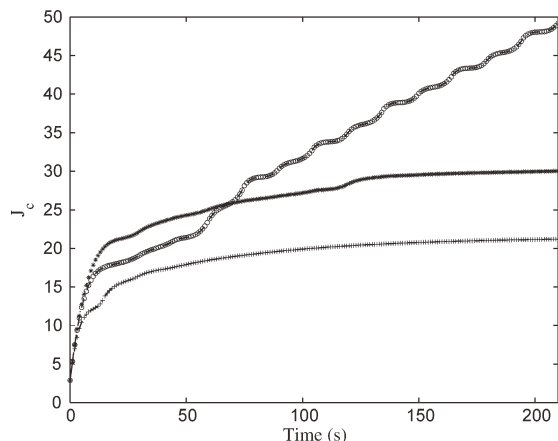**Figure 2. Diagram of chemical process example and fast-slow MPC architecture.**

Figure 3. Performance cost of each controller design based on Eq. 42a: the centralized LMPC design (dotted-solid line with plus), the slow LMPC design (dashed line with circles) with the fast proportional controller using $\Delta_f^P = 1$ s, and the slow LMPC design (solid line with asterisks) with the fast proportional controller using $\Delta_f^P = 0.001$ s.

controller, in the slow LMPC scheme that is combined with a fast proportional controller, is also implemented in a sample-and-hold fashion and its sampling time is denoted as Δ_f^P.

The numerical method that is used to integrate the full process model (i.e., singularly perturbed system with $\varepsilon > 0$) is explicit Euler with a fixed time step equal to 0.001 sec; this time step value was chosen to ensure stable numerical integration and sufficient accuracy. However, the numerical integration of the slow subsystem used in the slow LMPC scheme was carried out with explicit Euler with time step 0.1 sec because the slow subsystem is ε-independent. The numerical integration of the fast subsystem used in the fast LMPC scheme was carried out with explicit Euler with time step 0.001 sec owing to its fast dynamics. The optimization problems of each LMPC scheme are solved using the open source

interior point optimizer Ipopt. The Hessian is approximated by Quasi-Newton's method. Regarding the termination criteria and the maximum number of iterations, the values used by all simulations are 10^{-3} and 150, respectively.

The closed-loop performance of all LMPC schemes is illustrated in Figures 3 and 4. The trajectories of the slow LMPC scheme with the fast proportional controller in Figure 3 are evaluated based on Eq. 42a for the purpose of comparison. The performance costs in both figures clearly indicate that both the centralized LMPC and the fast-slow LMPC schemes stabilize the closed-loop process asymptotically to the steady state. We also note that both the fast LMPC and the slow LMPC in the composite fast-slow MPC design are able to stabilize the fast and slow dynamics of the singularly perturbed system asymptotically (Figure 4). On the other hand, under the setting of $\Delta_f^P = 1$ s, the slow LMPC scheme using a fast explicit controller is not able to drive the closed-loop system to the steady state. It causes oscillations of the closed-loop system around the steady state, which contributes to the increase of the performance cost with increasing simulation time (Figure 3). This problem can be resolved if the sampling time for the fast proportional controller is reduced to 0.001 seconds; specifically, Figure 3 shows that in this case the oscillations diminish and the closed-loop system converges to the final steady state gradually with a performance cost that is higher than the one of the centralized LMPC. Finally, it is important to note that we can not directly compare the optimal performance of the centralized LMPC scheme and that of the composite fast-slow LMPC scheme since they utilize different cost functions; see also remark 4 below.

Figures 5 and 6 show the simulation results comparing the computational speed between the centralized LMPC and the composite fast-slow LMPC. Since the explicit separation between the fast and slow dynamics reduces the dimension of the process dynamic model and allows increasing the step of numerical integration of the slow subsystem as well as reduces the number of manipulated inputs for the slow LMPC and the fast LMPC, the composite fast-slow LMPC computes the control action significantly faster compared to the centralized LMPC. Specifically, the results in Figures 5 and 6 indicate that the fast LMPC needs on average one
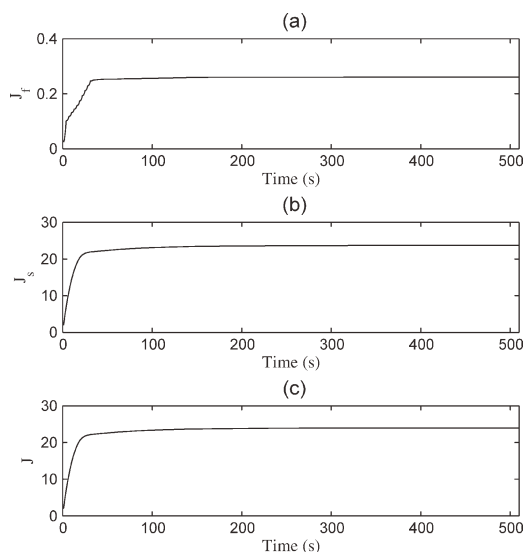

Figure 4. Fast-slow LMPC performance: (a) performance cost, J_f, of the fast LMPC, (b) performance cost, J_s, of the slow LMPC and (c) overall cost, J.
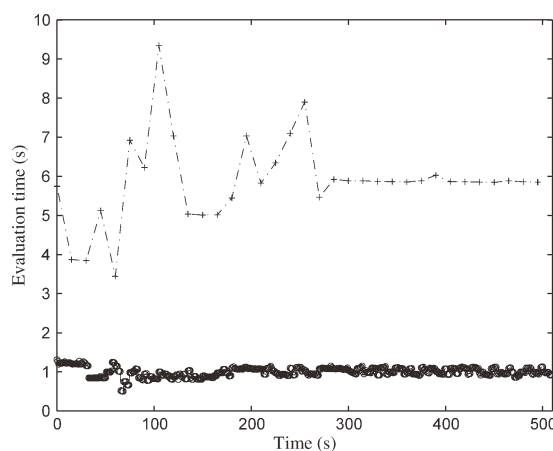

Figure 5. The total evaluation time needed for each evaluation of the control action by the centralized LMPC design (dashed-dotted line with plus) and by the fast LMPC of the fast-slow LMPC design (dashed line with circles).
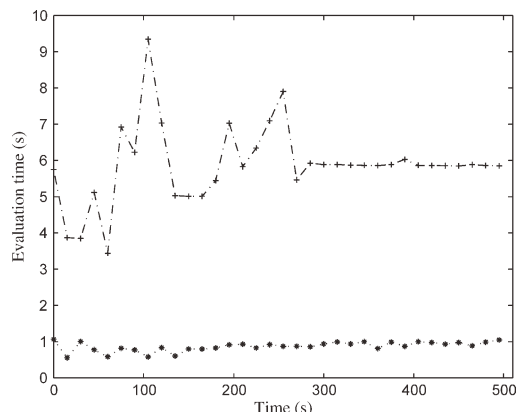
Figure 6. The total evaluation time needed for each evaluation of the control action by the centralized LMPC design (dashed-dotted line with plus) and by the slow LMPC of the fast-slow LMPC design (dotted line with asterisks).

second for the control action evaluation at each fast sampling time, and compared to the centralized LMPC, it is at least five times faster on average. Similarly, the slow LMPC is at least five times faster on average in evaluating its control actions at each slow sampling time compared to the time needed for the centralized LMPC.

Remark 4. *We note that in theorem 2 we establish that when the singular perturbation parameter is sufficiently small (but not zero), the value of the cost J computed on the basis of the singularly perturbed system under the proposed fast–slow LMPC design converges to the sum of the costs of the fast and slow closed-loop subsystems (ε = 0) under the same fast–slow LMPC design. This is an important point that establishes the well-posedness of the fast–slow MPC design for small ε. The reason we present the centralized LMPC application in the example is to compare the computational times between a brute-force design that neglects time-scale separation (centralized LMPC) and a design that accounts for time-scale separation (proposed fast–slow LMPC design). Even if we use J = J$_s$ + J$_f$ (the cost used in the fast–slow LMPC design) in the centralized LMPC, the resulting MPC still does not account for the time-scale separation and the resulting controller structure is different, and thus, a comparison of the centralized LMPC with the proposed fast–slow LMPC design would not be consistent.*

Conclusions

In this work, we focused on the theoretical development of a composite fast-slow LMPC architecture for nonlinear singularly perturbed systems in standard form and its application to a chemical process which consists of two continuous stirred tank reactors and a flash separator with recycle. The proposed fast-slow MPC design is decentralized in nature and enforces stability and near-optimality in the closed-loop singularly perturbed system provided the singular perturbation parameter is sufficiently small. Extensive simulations were carried out to compare the proposed architecture with existing centralized LMPC techniques from computational time and closed-loop performance points of view.

Literature Cited

1. Kokotovic P, Khalil HK, O'Reilly J. *Singular Perturbation Methods in Control: Analysis and Design*. London: Academic Press, 1986.
2. Christofides PD, Daoutidis P. Feedback control of two-time-scale nonlinear systems. *Int J Control*. 1996;63:965–994.
3. Kumar A, Daoutidis P. Nonlinear dynamics and control of process systems with recycle. *J Process Control*. 2002;12:475–484.
4. Christofides PD, Teel AR, Daoutidis P. Robust semi-global output tracking for nonlinear singularly perturbed systems. *Int J Control*. 1996;65:639–666.
5. Mayne DQ, Rawlings JB, Rao CV, Scokaert POM. Constrained model predictive control: stability and optimality. *Automatica*. 2000;36:789–814.
6. Mhaskar P, El-Farra NH, Christofides PD. Stabilization of nonlinear systems with state and control constraints using Lyapunov-based predictive control. *Syst Control Lett*. 2006;55:650–659.
7. Wogrin M, Glielmo L. *An MPC scheme with guaranteed stability for linear singularly perturbed systems*. In *Proceedings of the 49th IEEE Conference on Decision and Control*, Atlanta, GA, 2010:5289–5295.
8. Brdys MA, Grochowski M, Gminski T, Konarczak K, Drewa M. Hierarchical predictive control of integrated wastewater treatment systems. *Control Eng Pract*. 2008;16:751–767.
9. Van Henten EJ, J. Bontsema. Time-scale decomposition of an optimal control problem in greenhouse climate management. *Control Eng Pract*. 2009;17:88–96.
10. Chen X, Heidarinejad M, Liu J, Muñoz de la Peña D, Christofides PD. Model predictive control of nonlinear singularly perturbed systems: application to a large-scale process network. *J Process Control*. 2011;21:1296–1305.
11. Baldea M, Daoutidis P. *Control of integrated chemical process systems using underlying DAE models*. In: Biegler LT, Campbell S, Mehrmann V, editors. *Control and Optimization with Differential-Algebraic Constraints*. SIAM 2011.
12. Baldea M, Daoutidis P, Nagy ZK. Nonlinear model predictive control of integrated process systems. Presented at the NOLCOS, 8th IFAC Symposium on Nonlinear Control Systems, Bologna, Italy, 2010:1040–1045.
13. Lin Y, Sontag ED, Wang Y. A smooth converse Lyapunov theorem for robust stability. *SIAM J Control Optim*. 1996: 34:124–160.
14. Christofides PD, El-Farra NH. *Control of Nonlinear and Hybrid Process Systems: Designs for Uncertainty, Constraints and Time-Delays*. Berlin, Germany; Springer-Verlag, 2005.
15. Massera JL. Contributions to stability theory. *Ann Math*. 1956;64: 182–206.
16. Muñoz de la Peña D, Christofides PD. Lyapunov-based model predictive control of nonlinear systems subject to data losses. *IEEE Trans Aut Control*. 2008;53:2076–2089.
17. Christofides PD and Teel AR. Singular perturbations and input-to-state stability. *IEEE Tran Aut Control*. 1996;41:1645–1650.
18. Liu J, Muñoz de la Peña D, Christofides PD. Distributed model predictive control of nonlinear process systems. *AIChE J*. 2009;55: 1171–1184.
19. Liu J, Chen X, Muñoz de la Peña D, Christofides PD. Sequential and iterative architectures for distributed model predictive control of nonlinear process systems. *AIChE J*. 2010;56:2137–2149.
20. Christofides PD, Liu J, Muñoz de la Peña D. *Networked and Distributed Predictive Control: Methods and Nonlinear Process Network Applications. Advances in Induatrial Control Series*. London, England: Springer-Verlag, 2011.
21. Scattolini R. Architectures for distributed and hierarchical model predictive control—a review. *J Process Control*. 2009;19:723–731.
22. Stewart BT, Venkat AN, Rawlings JB, Wright SJ, Pannocchia G. Coorperative distributed model predictive control. *Syst Control Lett*. 2010;59:460–469.
23. Khalil HK. *Nonlinear Systems*, 2nd ed. NJ: Prentice Hall, 1996.